Evaluation of the sinking processes for high-pressure-gas cylinders

Heng-Sheng Lin[1,*], *Chien-Yu* Lee[1], *Chia-Jung* Lin[2], and *Ho-Chung* Fu[1]

[1]Department of Mold and Die Engineering, National Kaohsiung University of Applied Sciences, Kaohsiung 807, Taiwan
[2]Mosa Industrial Corporation, Huwei, Yunlin 632, Taiwan

Abstract. High-pressure-gas cylinders are used in broad applications. Cracks on the open end would occur during the riveting stage. Such forming defects are caused by excessive hardening, although the open end has been annealed with induction heating prior to the sinking operation. Therefore, a proper design for the sinking dies is essential to the forming production of the HPG cylinders. In this paper, two die-design concepts were examined which included the conventional design for six-stage sinking with fixed die radius, and the economic design for five-stage sinking with incremental die radii. Finite element software DEFORM 2D was used to investigate the two sinking schemes. The effect of the sinking schemes on the sinking load, strain distribution, and lip thickness were analysed. The results show that the economic five-stage sinking with a large increment of die radii can provide less strain hardening as compared to other sinking schemes. Although the forming load level is acceptable and the change of lip thickness is insignificant, the production cost of the five-stage scheme is still high. A more economic measure by sinking with one-stage rotary swaging can provide an alternative scheme with advantages of simple die design and saving the lead for annealing.

1 Introduction

High-pressure-gas (HPG) cylinders are used in broad applications such as food dispensers, air pistols, fire extinguishers and so on. The manufacturing process of the 8-gram HPG cylinder, as shown in Fig. 1, comprises blanking from steel coil and followed by deep-drawn into a slender tube in six-stage transfer stamping. The workpiece is then sunk and annealed with induction heating on its open end. The preform is further sunk with another six-stage transfer stamping, as shown in Fig. 2. The tube is subsequently milled on its open end and filled with high pressure gas and riveted to its completion. Some detailed manufacturing processes can be found in literature [1] for other examples of HPG cylinders.

Cracks on the open end would occur during the riveting stage. Such forming defects are caused by excessive hardening, although the open end has been annealed with induction heating prior to the sinking operation. Therefore, a proper design for the sinking dies is essential to the forming production of the HPG cylinders. Amirhosseini et al. [2] analyze

*Corresponding author: hslin@kuas.edu.tw

the nosing process of empty and foam-filled circular metal tubes on semispherical die, and Lu [3] studies the preform and loading rate in the tube nosing process by spherical die. Sheu and Su [4] investigate the cold nosing process for the aluminum conical milk can. Kwan [5] investigates the cold eccentric nosing process of metal tubes with an eccentric conical die from circular tube billets. Oba et al. [6] use two-step forming for improvement of forming limit in rotary nosing with relieved die for reduction of tube tip.

In this paper, two die-design concepts were examined which included the conventional design for six-stage sinking with fixed die radius, and the economic design for five-stage sinking with incremental die radii. Finite element software DEFORM 2D was used to investigate the two sinking schemes. The effect of the sinking schemes on the sinking load, strain distribution, and lip thickness were analysed. Finally the multi-stage sinking schemes were compared with the one-stage rotary swaging process by experimental verification.

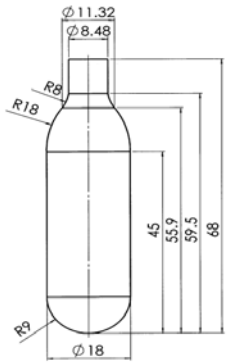

Fig. 1. Dimensions of HPG cylinder.

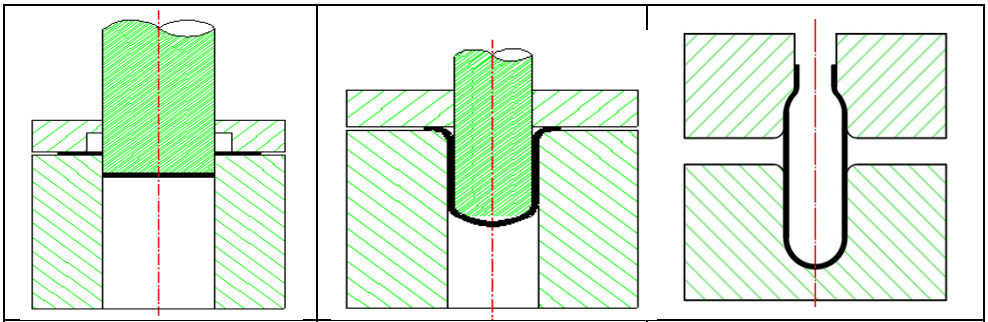

Fig. 2. Forming stages of HPG cylinders.

2 Methods

2.1 Sheet material

The sheet metal used was cold rolled steel SPCE of 0.8 mm thick. The flow stress of the sheet metal is shown in Fig. 3. The average yield strength σ_y was 160 MPa.

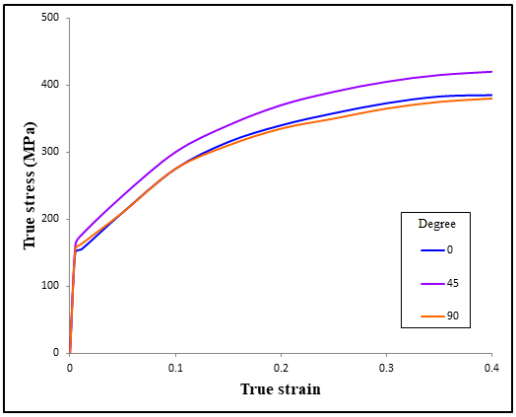

Fig. 3. Flow stress of SPCE steel sheet.

2.2 Sinking schemes

After the completion of deep drawing, one stage sinking and annealing, the workpiece's open end was to be sunk from 14.0 to 8.5 mm in its outer diameter. For the conventional six-stage sinking scheme, a sinking ratio of 0.92 was chosen, while for the economic five-stage sinking scheme, a sinking ratio of 0.90 was used. The target outer diameters used in both six-stage and five-stage sinking schemes are shown in Tables 1 and 2, respectively.

Table 1. Target outer diameters used in six-stage sinking scheme, sinking ratio 0.92.

	Stage 1	Stage 2	Stage 3	Stage 4	Stage 5	Stage 6
Outer diameter, mm	12.9	11.8	10.9	10.0	9.2	8.5

Table 2. Target outer diameters used in five-stage sinking scheme, sinking ratio 0.90.

	Stage 1	Stage 2	Stage 3	Stage 4	Stage 5
Outer diameter, mm	12.6	11.3	10.2	9.2	8.5

Die radii remain unchanged throughout each sinking stage in the conventional six-stage sinking scheme. However, die radii are reduced incrementally as sinking proceeds in the economic five-stage sinking schemes. Table 3 shows the die radii used in each stage of the respective sinking schemes. Increments from 0 to 9 mm were tested from the FE simulation. Fig. 4 shows the variations of die radius with outer tube half-diameter for a typical case of forming scheme "Incremental 1".

Table 3. Die radii used in each stage of forming schemes, unit: mm.

Forming schemes	Stage 1	Stage 2	Stage 3	Stage 4	Stage 5	Stage 6
Conventional 6	7	7	7	7	7	7
Incremental 0	7	7	7	7	7	
Incremental 1	11	10	9	8	7	
Incremental 3	19	16	13	10	7	
Incremental 5	27	22	17	12	7	
Incremental 7	35	28	21	14	7	
Incremental 9	43	34	25	16	7	

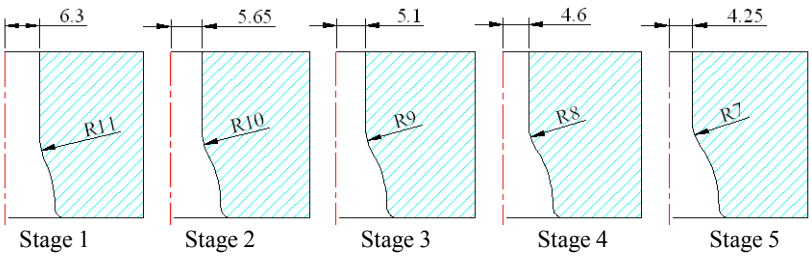

Fig. 4. Variations of die radius with outer tube half-diameter for forming scheme "Incremental 1".

2.3 FE simulation

Finite element software DEFORM was used in simulating all the sinking schemes. The 2D axis-symmetric module was chosen. The planar anisotropy of the sheet material was neglected. There were 5,000 elements used in meshing the workpiece, and all the forming tools were assumed to be rigid. Fig. 5 shows the schematic of the setup for the sinking operation. The stamping speed was fixed to 300 mm/s. Because the tribological behavior of the process was not the main trust of this work, friction factors at the interfaces between the tool and workpiece were fixed to 0.05.

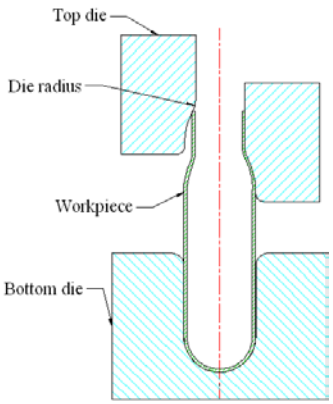

Fig. 5. Setup for the sinking operation, left: before sinking; right: at the lower dead point of sinking.

3 Results

3.1 Sinking load/stress

The sinking load occurring on the open end of tube should not exceed to cause distortion on the tube body which nests inside the bottom die. To ensure that the tube body is not distorted during sinking, the axial stress on the tube body should not exceed the yield stress of workpiece. Therefore, the sinking load obtained from the simulation is first divided by the cross-sectional area of tube body to obtain the axial sinking stress σ_s. The sinking stress is further non-dimensionalized by dividing by the initial yield stress σ_y of the sheet metal. When the value σ_s / σ_y is much greater than unity, there is possibility of distortion on the tube body.

The sinking stresses for both the conventional six-stage and the economic five-stage schemes are shown in Fig. 6. The sinking stress increases as the forming stage proceeds,

attributed to the increase of strain hardening in the sinking zone. The stress level is higher with the economic five-stage scheme because of greater amount of deformation was used for the respective sinking stages.

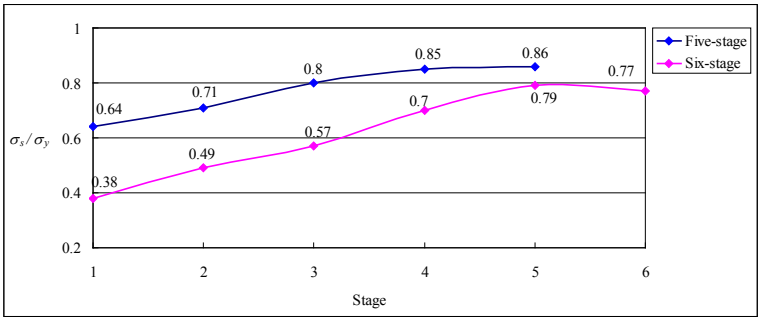

Fig. 6. Sinking stresses for both the conventional six-stage and the economic five-stage schemes.

Fig. 7 shows the sinking stresses for the five-stage schemes of various increments of die radius. The sinking stress increases as the increment of die radius increases. This is caused by the increasing frictional stress exerting on a larger contact interface between the die face and workpiece when the die radius becomes larger. Some values are greater than unity for the forming schemes with increments of die radius larger than 3 mm. Overall, the sinking stress shown in Fig. 7 are acceptable without causing distortion on the tube body. The tube body has experienced certain amount of strain hardening during the prior deep drawing stages. Therefore the yield stress on the tube body should be much higher than the initial yield stress 160 MPa of the sheet metal used in the calculation. The forming stress of Stage 5 is slightly less than that of Stage 4. This is because the sinking amount decreases substantially at the final stage as compared to that of Stage 4, although the sinking ratio remains constant throughout the sinking schemes.

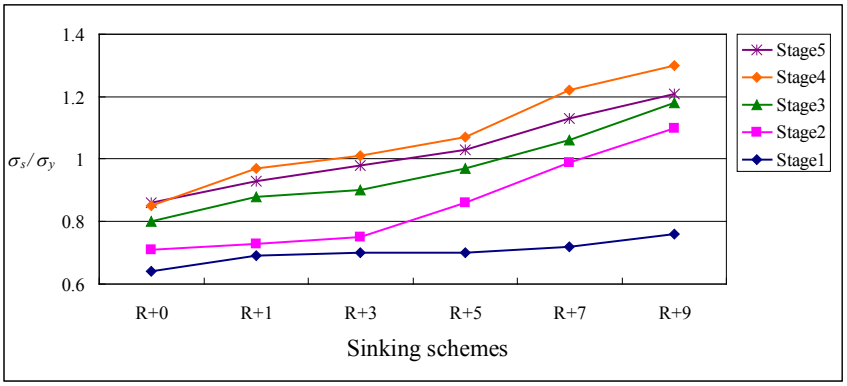

Fig. 7. Sinking stresses for the five-stage schemes of various increments of die radius.

3.2 Distribution of effective strain

Fig. 8 shows the distributions of effective strain at the final stage of selective sinking schemes. The maximum effective strain occurs on the tube inner surface and the value decreases as the die radius increases. This indicates that the strain inhomogeneity decreases with a small die inclusion angle in sinking with a large die radius [7]. High strain level is unfavourable, according to the field experience, because the sinking zone would become susceptible to crack formation in the subsequent riveting operation.

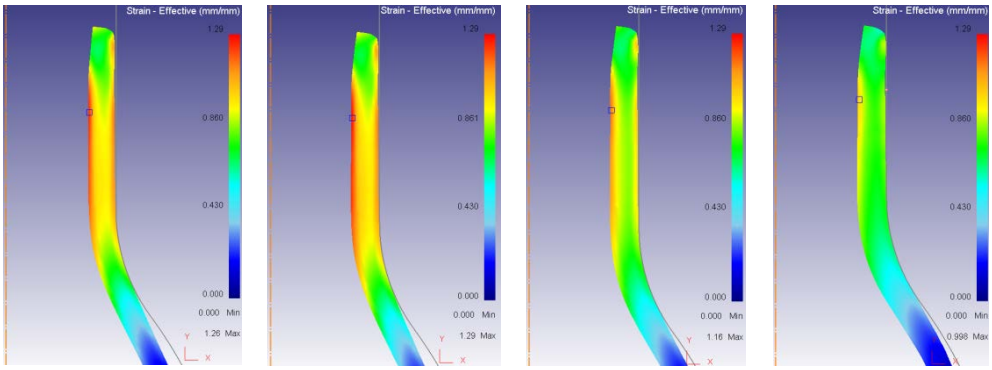

(a) Conventional 6 (b) Incremental 0 (c) Incremental 3 (d) Incremental 9

Fig. 8. Distributions of effective strain at the final stage of various sinking schemes.

Fig. 9 shows the distributions of effective strain along the radial direction at Stage 5 for the economic sinking schemes. The radial position is normalized by the outer radius of the sunk tube. The distributions show a monotonic decrease of effective strain as the increment of die radius increases. The phenomenon observes that the strain level, i.e. deformation inhomogeneity [7] decreases, as the die inclusion angle increases. This trend indicates that using a large increment of die radius can obtain a less hardened sunk tube.

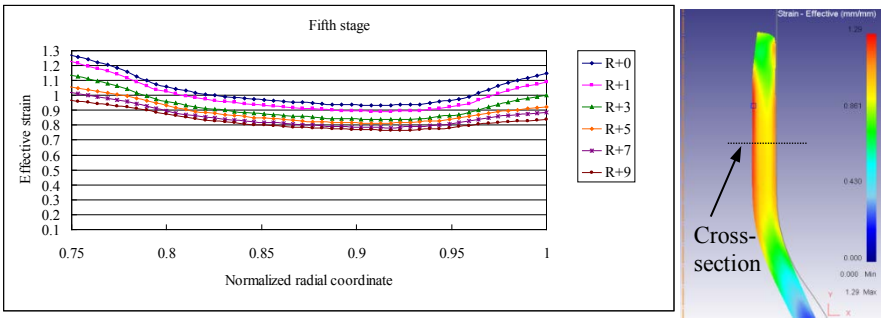

Fig. 9. Distributions of effective strain at Stage 5 of economic sinking schemes.

3.3 Lip thickness

Lip thickness increases during the sinking process. It is the primary straining direction as compared to the axial straining. Fig. 10 shows the increase of lip thickness of respective forming schemes, and the amount decreases sharply at the final stage, attributed to the accumulated strain hardening from the sinking operation. The six-stage sinking scheme exhibits a mild increase of lip thickness because of a large sinking ratio 0.92 was used for the respective stages. Fig. 11 shows the final lip thickness of respective sinking schemes. The lip thickness is the largest in sinking with an increment of die radius of 9 mm, followed by 7 mm, and so on. This is due to less strain level was generated in sinking with a large die radius, i.e. a small die inclusion angle. The analyses for the lip thickness all indicates that the variations with the change of die design are not significant. This guarantees that the amount of surface machining in the original process design remains valid.

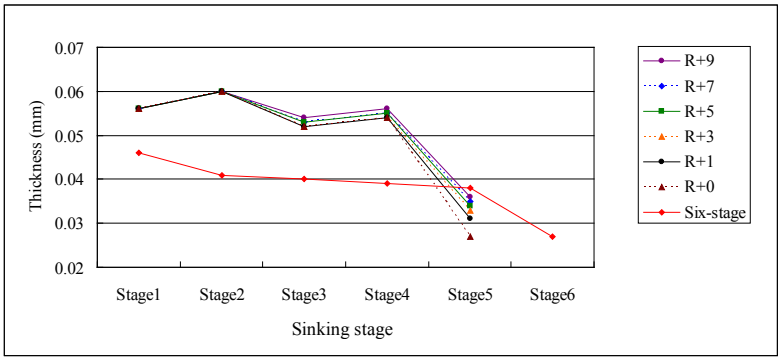

Fig. 10. Increase of lip thickness of respective sinking schemes.

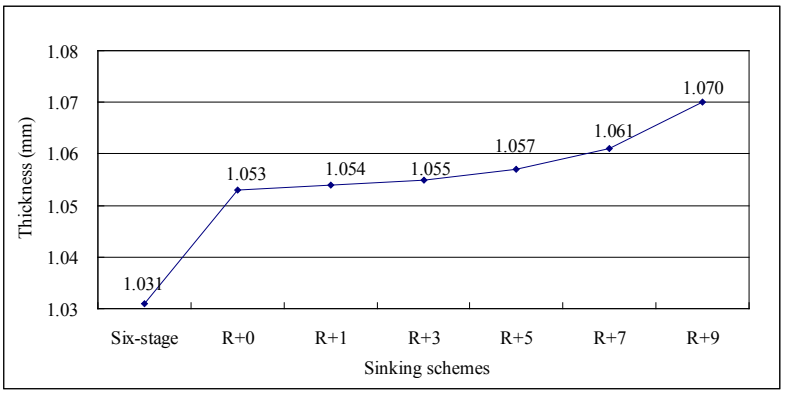

Fig. 11. Final lip thickness of respective sinking schemes.

4 Discussions

In Section 3, two die-design concepts are examined which include the conventional design for six-stage sinking with fixed die radius, and the economic design for five-stage sinking with incremental die radii. The results of the FE analysis show that economic five-stage with a large increment of die radii can provide less strain hardening as compared to other sinking schemes. Although the forming load level is acceptable and the change of lip thickness is insignificant, the production cost of the "economic" five-stage scheme is still high. The energy used in conduction heating, the effort in pickling the oxidation, and the maintenance of the multi-stage dies, still render the sinking scheme by transfer stamping not a lean and green manufacturing method.

A more economic measure by sinking with one-stage rotary swaging has been attempted by Lin et al. [8]. Figure 12 shows a typical hardness distribution along the axial direction for sinking with an un-annealed tube (preform). There is no significant difference between the un-annealed preform and the swaged workpiece, which indicates the feasibility of sinking with un-annealed preform. The distribution also shows that the variation of hardness number is less on the outer surface than that of inner surface. A similar trend is also observed in the FE analysis of the distribution of effective strain that the hardening level is higher on tube inner surface than that of outer surface, as shown in Fig. 9.

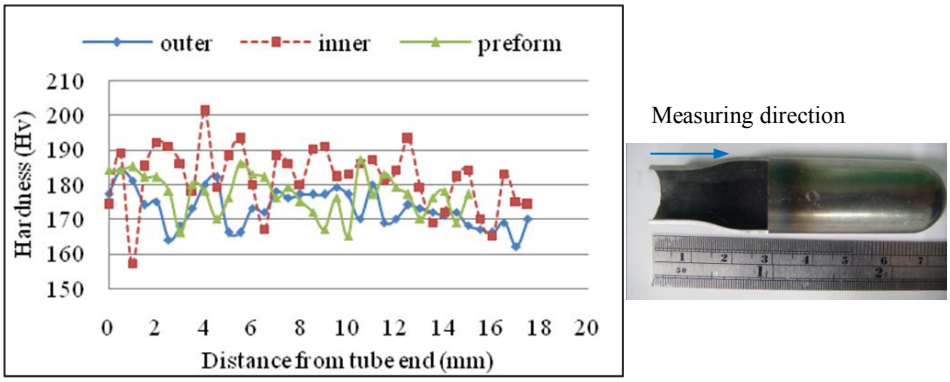

Fig. 12. Hardness distribution of sinking of one-stage rotary swaging with un-annealed preform. [8]

5 Conclusions

Two die-design concepts were examined in this work which included the conventional design for six-stage sinking with fixed die radius, and the economic design for five-stage sinking with incremental die radii. Finite element software DEFORM 2D was used to investigate the two sinking schemes. The results show that the economic five-stage sinking with a large increment of die radii can provide less strain hardening as compared to other sinking schemes. Although the forming load level is acceptable and the change of lip thickness is insignificant, the production cost of the five-stage scheme is still high. A more economic measure by sinking with one-stage rotary swaging can provide an alternative scheme with advantages of simple die design and saving the lead for annealing.

Acknowledgements

The authors acknowledge Mosa Industrial Corporation in providing the samples.

References

1. *ASM Metals Handbook*, Volume 14, Forming and Forging (1989)
2. S.G. Amirhosseini, A. Niknejad, N. Setoudeh, Trans. Nonferrous Met. Soc. China **27**, 1976 (2017)
3. Y.H. Lu, Comput. Methods Appl. Mech. Engrg. **194**, 2839 (2005)
4. J.J. Sheu, H.H. Su, Proceedings of the 2009 IEEE IEEM, 2319
5. C.T. Kwan, J. Mater. Process. Technol. **140**, 530 (2003)
6. W. Obaa, Y. Imaizumia, S. Kajikawaa, T. Kubokia, Procedia Eng. **207**, 1743 (2017)
7. W.F. Hosford, R.M. Caddell, *Meral Forming, Mechanics and Metallurgy*, 3rd edn. Cambridge University Press, UK (2007)
8. H.S. Lin, C.J. Lin, Y.C. Hsu, J.H. Lee, B.Y. Lee, Y.C. Chen, Steel Res. Int. **81**, 576 (2010)